EFFECT OF TRANSVERSE NORMAL STRESS ON MODE II FRACTURE TOUGHNESS IN FIBER COMPOSITES

Qida Bing*, C.T. Sun* [C.T. Sun]: sun@purdue.edu
***Purdue University, W. Lafayette, Indiana, USA**

Keywords: *Polymer-matrix composites, mode II fracture toughness, transverse normal stress*

Abstract

Effect of transverse normal stress on mode II fracture toughness of unidirectional glass fiber reinforced composites was studied experimentally and numerically. New mode II fracture tests using off-axis specimens with a through thickness crack were conducted on the S2/8552 glass/epoxy composite. The finite element method was employed to perform stress analyses from which mode II fracture toughness was extracted. In the analysis, crack surface contact friction effect was considered. It was found that the transverse normal compressive stress has significant effect on mode II fracture toughness of the composite. Moreover, the fracture toughness measured using the off-axis specimen was found to be quite different from that evaluated using the conventional end notched flexural (ENF) specimen in three-point bending. It was found that mode II fracture toughness cannot be characterized by the crack tip singular shear stress alone; non-singular stresses ahead of the crack tip appear to have substantial influence on the apparent mode II fracture toughness of the composite.

1 Introduction

Matrix cracking and interlaminar cracking are key failure modes in laminated composite structures. For this reason fracture behavior in composites has drawn much attention from composites researchers who have investigated various methods for characterizing this property. The end notch flexural (ENF) specimen under three-point-bending or four-point-bending is the most popular method for testing mode II interlaminar fracture toughness in composites mainly because of its simplicity [1-4]. In view of the highly nonlinear stress-strain curve in shear in most polymeric composites, the validity of the fracture toughness data obtained from the ENF test method remains an open question. It is well known that the presence of transverse compressive stress σ_{22} has a significant effect on the shear strength τ_{12} of unidirectional fiber reinforced composites [5-6]. Therefore, it is reasonable to surmise that a transverse compressive stress σ_{22} in the composite ahead of the crack tip may affect mode II fracture toughness as well since mode II fracture is driven by shear stress σ_{12}.

In this paper, a brick-shaped off-axis composite specimen with a partial crack created along the fiber direction is employed to produce mode II fracture in a unidirectional fiber composite. The advantage of using off-axis specimen with uniaxial compressive loading to produce a pure mode II fracture is that a combined state of stress along the crack path is generated. By changing the off-axis angle of the specimen, different levels of compressive transverse stress ahead of the crack tip can be generated and its effect on fracture toughness studied. Moreover, the distribution of the crack driving shear stress σ_{12} ahead of the crack tip in the off-axis specimen is found to be quite different from that in the ENF specimen. This difference helps to explain why the fracture toughnesses obtained from these two specimens are different.

2 Materials and Specimen Preparation

A 48-ply S2/8552 glass/epoxy laminate was manufactured by hand lay-up and cured in an autoclave under the recommended vacuum, heating and pressure cycle. The cure temperature was 170°C (350°F).

The edge cracked specimen was prepared following a procedure as depicted in Fig 1. The through-the-thickness edge crack along the fiber direction was created by forcing a razor blade into the edge of the cured laminate to produce mode I cracking. The off-axis specimen was then cut out by using a water jet cutting machine.

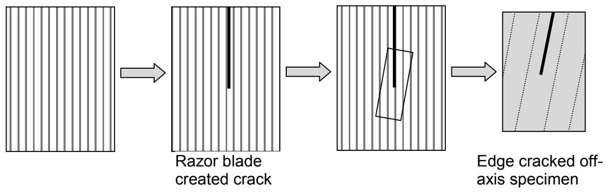

Fig. 1. Preparation of edge cracked off-axis specimen

The edge cracked specimens were prepared for off-axis angles of 5°, 10°, 20°, 30°, and 40°. The nominal specimen dimensions were 15mm wide, 20mm long and 4mm thick with 10mm nominal crack length. Both specimen ends were polished with grit 120 and grit 1200 sand papers and special effort was made to make sure that both specimen ends were parallel to each other. A crack propagation gage TK-09-CPB02-005 from Vishay Micro-Measurements™ was mounted on the specimen surface ahead of the crack tip to record the crack propagation history as shown in Fig. 2.

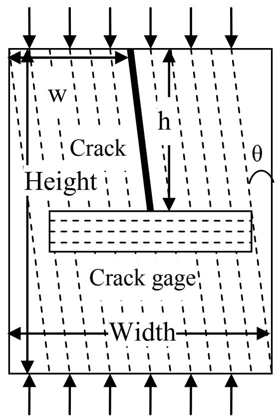

Fig. 2. Edge cracked off-axis specimen with off-axis angle θ

Fig. 2 also shows the dimensions of edge cracked off-axis specimen employed in finite element analysis, where *h* is the distance along the loading direction from the crack tip to the specimen end surface. It is noted that for the 40 degree off-axis specimen, the specimen width was doubled to allow enough room for crack propagation.

3 Static Fracture Tests

Static compression tests were performed on an MTS machine using these edge cracked off-axis specimens at 0.005mm/sec stroke speed. A self-adjusting system [7-8] was used in the compression tests in order to avoid potential bending moment. Lubricant was applied between the specimen and the loading element surface to minimize contact friction in all the tests. The crack gage was connected to a circuit as shown in Fig. 3. to record the crack propagation history. The sampling rate of data acquisition was 500Hz.

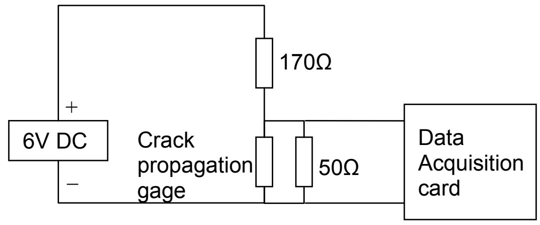

Fig. 3. Circuit of crack propagation gage

Load-displacement relations and histories of crack propagation for different off-axis specimens were recorded in experiments. Fig. 4 shows a typical load-displacement relation and crack extension history for a 10° off-axis specimen. It was observed that 5° and 10° off-axis specimens continued to carry load after initial crack extension, while the crack became unstable at the peak load in specimens with off-axis angles larger than 10°. The average crack propagation speed obtained from the measured crack extension data was found to be less than 1mm/sec. The critical load at which the first strand in the crack gage was broken was used to extract the critical energy release rate (fracture toughness) for each specimen with the aid of the finite element analysis as described in Section 5.

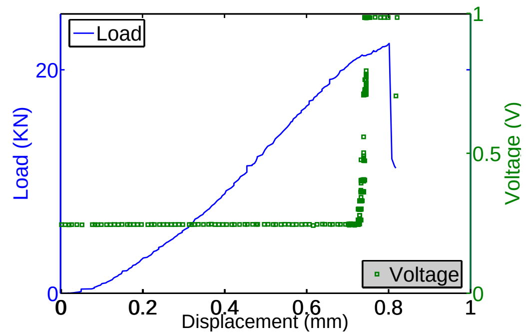

Fig. 4. Load and crack propagation history of 10° specimen

4 Static Coefficient of Friction of Crack Surface

In order to consider the effect of frictional contact of crack surfaces, the static coefficient of friction of the crack surfaces must be determined prior to performing the finite element analysis. A setup as shown in Fig. 5 was designed to measure the coefficient of friction of crack surfaces. Two pieces of a broken specimen after total fracture were placed on an MTS machine. The lower piece was gripped by the hydraulic grip and the upper piece was subjected to a compressive load P applied through a loading element with a smooth surface. When the horizontally applied force F reached a critical value the sliding between the two parts of the broken specimen occurred. The coefficient of friction of crack surfaces was then obtained from the relation $\mu = F / P$. The average coefficient of friction was found to be 0.403(±0.049) at the applied load P around 445N. It is noted that the coefficient of fraction of crack surfaces is constant with applied load up to 445N.

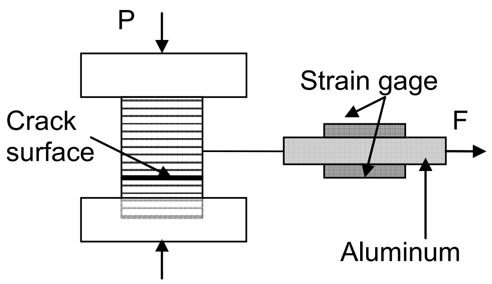

Fig. 5. Setup for measuring coefficient of friction

5 Elastic Finite Element Analysis

The finite element method is employed to extract the fracture toughness from the experimental data. The edge-cracked off-axis specimen of S2/8552 composite is modeled as 2-D orthotropic elastic solid in a state of plane stress using the commercial FEA package ABAQUS™. The 4-node plane stress quadrilateral element is used to mesh the specimen and elastic 'Lamina' material in ABAQUS™ is used to model material properties [7, 9]. The loading elements in the experiments are made of tungsten carbide which has a very high Young's modulus (420GPa) and, thus, are modeled as rigid bodies. Fig. 6 shows the assembly of an edge-cracked off-axis specimen in compression in the FE analysis. A pair of contact elements is used to model the interaction between the two crack surfaces. The tangential behavior of interaction is defined with coefficient of friction at 0.403 and the normal behavior is 'hard' contact which means no penetration is allowed. Ahead of the crack tip tie constraints are employed to bond two surfaces together. Frictionless interaction is used to model the interactions between the rigid loading surfaces and the end surface of the off-axis specimen. A fine uniform mesh with the element size of 4×10^{-3}mm is created around the crack tip. This mesh is found to be sufficient to obtain converged solutions. About 36000 elements are used to model the off-axis specimen.

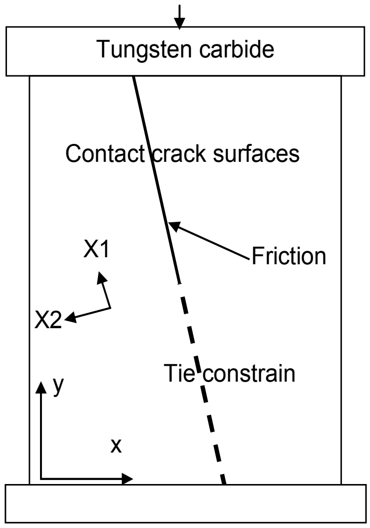

Fig. 6. Assembly of edge cracked off-axis specimen in compression

The finite element model is used to calculate the mode II energy release rate following a two-step procedure proposed by Sun and Qian [10] for bi-material interfacial cracks. By including the friction term in the virtual crack closure method they calculate the mode II energy release rate as,

$$G_{II} = \frac{1}{2\Delta a}(NFORC1 - \mu \times NFORC2) \times \Delta u \qquad (1)$$

where *NFORC1* is the nodal force at the crack tip parallel to the crack surface before crack extension of Δa, Δu is the relative displacement (parallel to the crack surface) after crack extension of the two nodes resulting from the splitting of the crack tip, μ is the coefficient of friction of the crack surfaces, *NFORC2* is the nodal force normal to the crack surface at the crack tip. In general, the $\mu\times$*NFORC2* is very small in homogeneous solid.

As required by the analysis methods, the nodal release on the crack surfaces is employed to simulate the forward crack propagation. After the load is applied on the tungsten carbide, a separation between the two tied nodes at the crack tip is allowed to simulate crack propagation over the distance of one element size while keeping the rigid loading body fixed as the boundary condition.

6 Fracture Mode and Crack Surface Friction

Fig. 7 shows the distribution of transverse normal (to the fibers) stress σ_{22} on the crack surface in the 20° off-axis specimen calculated with crack surface friction. The stress distribution clearly shows that the crack surfaces near the crack tip are under compression and thus only mode II loading is present in the off-axis specimen.

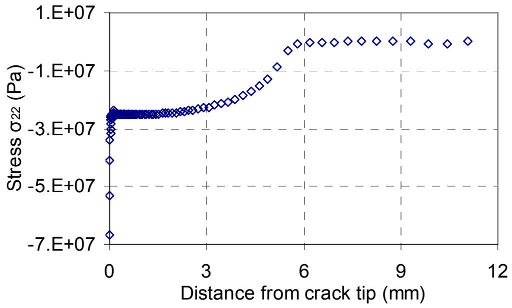

Fig. 7. Stress distribution of σ_{22} on the crack surface of 20° specimen

In order to determine the mode II fracture toughness, elastic FE analyses are performed with specimen dimensions and experimentally obtained critical loads. From Eq. 1 mode II fracture toughnesses are obtained for different off-axis angles. Fig. 8 shows the average mode II fracture toughnesses as well as standard deviations obtained from the data for different off-axis angles. In the same figure, toughness values calculated without considering friction are also presented. It is found that mode II fracture toughness increases as off-axis angle increases and that crack surface friction tends to decrease the rate of increase of mode II fracture toughness as off-axis angle increases. The most interesting finding is that mode II fracture toughness is not a constant value as expected. In other words, the energy release rate (or equivalently the stress intensity factor) alone is not sufficient to characterize mode II fracture toughness in the composite.

7 Effect of Transverse Compressive Stress σ_{22} on Mode II Fracture Toughness

It is well known that transverse compressive stress σ_{22} can significantly increase the longitudinal shear strength (τ_{12}) of unidirectional fiber reinforced composites [5-6]. It is noted that the amount of transverse normal stress σ_{22} in an off-axis specimen under compressive loading increases as the off-axis angle increases. The variation of σ_{22} ahead of the crack tip may influence the fracture condition in the cracked off-axis specimen.

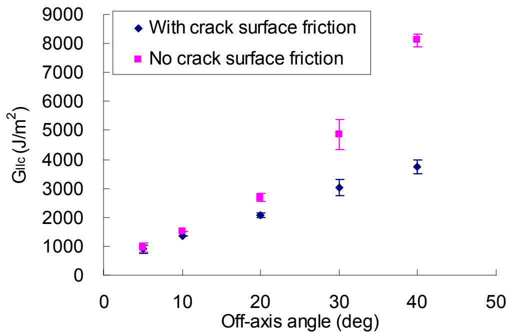

Fig. 8. Mode II fracture toughness for different off-axis angels

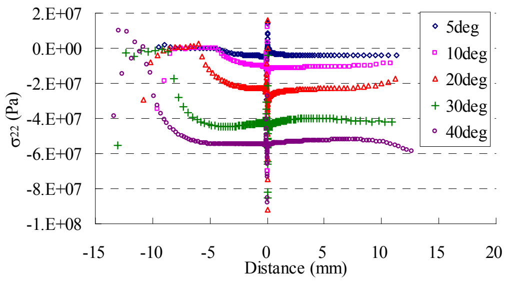

Fig. 9. Stress distribution of σ_{22} along the crack surface direction (0 is crack tip)

Fig. 9 shows the distributions of σ_{22} along the crack plane behind and ahead of the crack tip for different off-axis angles. It is evident that the level of compressive normal stress near the crack tip increases as the off-axis angle increases.

Fig. 10 shows the plot of the relation between mode II fracture toughness and compressive stress σ_{22}. In the plot, average transverse compressive stresses σ_{22} is calculated over the region ahead of the crack tip. The plot clearly shows that there is a significant effect of the compressive stress σ_{22} on mode II fracture toughness. The relation between mode II fracture toughness and σ_{22} can be represented well by a linear function as,

$$G_{IIC} = k\sigma_{22} + G_{IIC0} \quad (2)$$

$$k = 5.65 \times 10^{-5} \frac{J}{m^2 P_a} \quad (3)$$

$$G_{IIC0} = 713 \frac{J}{m^2} \quad (4)$$

where the parameter k defines how the compressive transverse stress affects the fracture toughness of S2/8552 glass/epoxy composite and G_{IIC0} is the projected fracture toughness when transverse normal stress is absent.

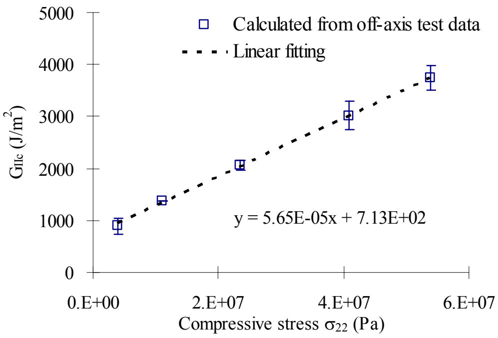

Fig. 10. Effect of compressive stress σ_{22} on mode II fracture toughness

8 Comparison with Results of ENF Specimen in three point bending

The ENF specimen in three-point bending is a very popular method for measuring interlaminar fracture toughness in fiber composites. For the purpose of comparison, ENF specimens were also tested. The ENF specimens were prepared following a similar procedure as employed for making off-axis specimens. It is noted that the height direction of the ENF specimen is parallel to the plane of the composite panel and the width is the thickness of the panel. The specimen is 3.82mm wide which is the thickness of the 48-ply laminate, and 5.62mm thick with 25mm long crack. Two tests were performed with half span length of 50mm.

Finite element analyses including the crack surface friction effect are performed by using failure loads from the ENF test results. The average mode II fracture toughness from modified crack closure method is obtained to be 2545.9J/m^2 with a standard deviation of 173.2J/m^2.

Three-point bending tests with ENF specimens having an interlaminar crack created at the mid plane of the laminate were performed as well. The specimens are around 20mm wide and 4mm thick with 20mm long crack in the middle plane of thickness direction. Two tests were performed with half span lengths at 40mm and 50mm, respectively. The average mode II fracture toughness from ENF specimens with an interlaminar crack obtained from the FE analysis is 1615.2J/m^2 (standard deviation is 227.8J/m^2). It is interesting to note that there is a large difference between the fracture toughnesses obtained from ENF specimens with an interlaminar crack and a through-the-thickness crack, respectively. The reason of this larger fracture toughness of through-thickness crack may lie in the fact that the fiber bridging is less severe in the interlaminar crack.

It should be noted that in the ENF test, transverse normal stress is basically nil. For the purpose of comparison we obtain the projected toughness value (713J/m^2) at vanishing transverse compressive stress from off-axis test results shown in Fig. 10. The fracture toughness (2545.9J/m^2) obtained from ENF test method is more than three times higher than that estimated based on the off-axis test results.

The large difference between the results of the ENF and off-axis specimens needs explanations. Since the transverse normal stress effect has been eliminated by using the projected value as described above, the other possible factor is the T stress (or nonsingular stress) effect [11]. Since polymeric fiber composites exhibit appreciable nonlinear stress-strain behavior, the nonsingular part of the shear stress ahead of the crack tip may significantly influence the fracture toughness. For this purpose, we perform elastic FE analyses on ENF and off-axis specimens with respective loads that produce same mode II energy release rate of 2545.9J/m^2. Of course, a different energy release rate value can be selected without loss of generality. Fig. 11 shows the comparison of shear stress distributions ahead of the crack tip for 5^o off-axis specimen loaded at 55.1KN, 10^o off-axis specimen at 27.5KN, and the ENF specimen, all of which produce mode II energy release rate of 2545.9J/m^2. Note that the vertical axis in Fig. 11 is shear stress multiplied by square root of the distance from the crack tip and, thus, the stress intensity factor is given at x = 0.

From Fig. 11 it is found that, although all three specimens yield the same stress intensity factor, the non-singular stress in the off-axis specimens is quite different from that in the ENF specimen. In fact the magnitude of the nonsingular part of the shear stress in off-axis specimens is much greater than that in the ENF specimen. This high nonsingular stress adds to the crack driving force in less brittle materials. This explains why the mode II fracture toughness in the composite obtained from off-axis specimens is much smaller than that from the ENF specimen when transverse normal stress in absent. This result indicates that linear elastic fracture mechanics (LEFM) is not adequate for characterizing Mode II fracture toughness in polymeric fiber composites.

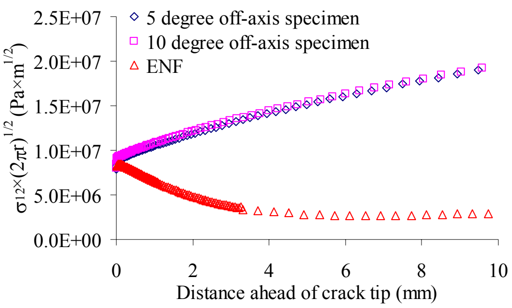

Fig. 11. Elastic shear stress distributions ahead of crack

9 Conclusions

A new method by utilizing off-axis specimens for mode II fracture test on polymeric fiber reinforced composite materials has been investigated. The advantage of this method is it gives ability to study the effects of crack surface friction and transverse compressive stress σ_{22} on mode II fracture toughness of fiber reinforced composite materials. It was found that the transverse compressive stress ahead of the crack tip can greatly increase the mode II fracture toughness of polymeric composites. It was also found that the nonsingular part of the shear stress has a significant influence on the apparent mode II fracture toughness indicating that LEFM is not sufficient to characterize this toughness property. This finding helps to explain why the mode II fracture toughness obtained from the ENF specimen and that from off-axis specimens show a substantial difference.

References

[1] Carlsson L.A. and Pipes R.B. "*Experimental characterization of advanced composite materials*". Prentice-Hall, Inc., Englewood Cliffs, New Jersey, pp 167-180, 1987.

[2] Tsai J.L., Guo C. and Sun C.T. "Dynamic delamination fracture toughness in unidirectional polymeric composites". *Compos Sci Technol*, Vol. 61, pp 87-94, 2001.

[3] Sun X. and Davidson B.D. "A direct energy balance approach for determining energy release rates in three and four point bend end notched flexure tests". *Int J Fracture*, Vol. 135, pp 51-72, 2005.

[4] Martin R.H. and Davidson B.D. "Mode II fracture toughness evaluation using four point bend, end notched flexure test". *Plast Rubber Compos*, Vol. 28, No. 8, pp 401-406, 1999.

[5] Sun C.T. "Strength analysis of unidirectional composites and laminates". *Comprehensive Composite Materials*, ed. Kelly, A. and Zweben, C. Elsevier Science, Ltd., Oxford, pp 641-666, 2000.

[6] Swanson S.R., Messick M.J. and Tian Z. "Failure of Carbon/Epoxy Lamina Under Combined Stress". *J COMPOS MATER,* Vol. 21, pp 619-630, 1987.

[7] Tsai J. and Sun C.T. "Constitutive model for high strain rate response of polymeric composites". *Compos Sci Technol*, Vol. 62, pp 1289-1297, 2002.

[8] Bing Q. and Sun C.T. "Modeling and testing strain rate-dependent compressive strength of carbon/epoxy composites". *Compos Sci Technol*, Vol. 65, No. 15-16, pp 2481-2491, 2005.

[9] Sun C.T. and Han C. "A method for testing interlaminar dynamic fracture toughness of polymeric composites". *Compos Part B*, Vol. 35, pp 647-655, 2004.

[10] Sun C.T. and Qian W. "A treatment of interfacial cracks in the presence of friction". *Int J Fracture*, Vol. 94, pp 371-382, 1998.

[11] Anderson T.L. "*Fracture Mechanics*". 2nd edition, CRC Press, 1995.

Acknowledgement

This work was supported by ONR grant No. N00014-1-0552. Dr. Yapa D. S. Rajapakse was the program manager.